Biomechanics of DNA structures visualized by 4D electron microscopy

Ulrich J. Lorenz and Ahmed H. Zewail[1]

Physical Biology Center for Ultrafast Science and Technology, Arthur Amos Noyes Laboratory of Chemical Physics, California Institute of Technology, Pasadena, CA 91125

Contributed by Ahmed H. Zewail, January 10, 2013 (sent for review December 3, 2012)

We present a technique for in situ visualization of the biomechanics of DNA structural networks using 4D electron microscopy. Vibrational oscillations of the DNA structure are excited mechanically through a short burst of substrate vibrations triggered by a laser pulse. Subsequently, the motion is probed with electron pulses to observe the impulse response of the specimen in space and time. From the frequency and amplitude of the observed oscillations, we determine the normal modes and eigenfrequencies of the structures involved. Moreover, by selective "nano-cutting" at a given point in the network, it was possible to obtain Young's modulus, and hence the stiffness, of the DNA filament at that position. This experimental approach enables nanoscale mechanics studies of macromolecules and should find applications in other domains of biological networks such as origamis.

nanomechanical properties | ultrafast electron microscopy

In macroscopic engineering of structures, the nature of mechanical motions is critical for their robustness and function, as evidenced in the design of colossal structures from the Pyramids to the Eiffel Tower. Our modern-day quest for miniaturization has led to the construction of ever more sophisticated nanoscale structures and devices, defining new frontiers in materials science and nanotechnology (1). Biological nanostructures and nanomachines have also attracted considerable interest, and efforts are directed at harnessing their power for the construction of devices with novel functions (2). A prominent example is DNA nanotechnology, which exploits the fact that DNA can be programmed and made to self-assemble into complex structures and functional devices (3–5). For all of these structures and applications, the need continues for the development of suitable tools that enable the visualization of these nanoscopic systems and the control of their properties.

Progress has been made in the development of techniques involving single-molecule stretching and nano-indentation (6–9) to access the intrinsic force of biological structures. Recently, ultrafast electron microscopy (UEM) has been developed to directly visualize nanomechanical motions in space and time (10, 11). The applications span a range of materials properties, including the drumming of a thin graphite membrane (12), vibrations of carbon nanotubes (13), molecular nanocrystals (14), and bimetallic nanostructures fabricated with nanoelectromechanical systems technology (15). Although it appears promising to extend these techniques to the investigation of the material properties of individual biological nanostructures, several additional challenges had to be overcome.

In UEM experiments, a short laser pulse is used to excite the specimen and trigger coherent motions, which are probed with the electron pulses. However, many biological systems do not possess a suitable chromophore and may be susceptible to photodamage, as we expect for the DNA nanostructures investigated here (16). The dynamics are usually recorded in stroboscopic mode, i.e., a single time frame is obtained by repetitive recording (here, on the order of 10^4 individual experiments are averaged), and bleaching of the chromophore and accumulated damage resulting from excited-state reactions and laser-induced heating may severely limit the feasibility of direct imaging. Moreover, for biological structures of nanoscale thickness that do not absorb significant amounts of light, the question remains of how mechanical oscillations would be induced and if they would be of sufficiently large amplitude.

We describe our in situ visualization of the mechanical properties of a DNA nanostructure and the direct measurement of its stiffness from the induced vibrational oscillations. The structures were created by stretching DNA over a hole embedded in a thin carbon film. Using an electron beam, we severed several of the filaments connecting it to the carbon support to obtain a free-standing structure that exhibits oscillations of sufficiently large amplitude and also lends itself to vibrational analysis. The mechanical motion is induced through an efficient methodology that does not rely on the absorption properties of DNA and should be transferrable to other biological studies. We use a visible laser pulse to trigger a short burst of strain in the carbon substrate, which results in a sufficiently broad vibrational frequency spectrum, and in turn impulsively excites the oscillations of the nanostructure. This microscopic approach is analogous to using a hammer blow to excite the eigenmodes of a suspended macroscopic object whose oscillations are subsequently recorded as a function of time for deducing mode shapes and eigenfrequencies (17).

Results and Discussion

Preparation of DNA Nanostructures. When a solution of λ-DNA is left to dry on a holey carbon film, the 48,502-bp bacteriophage DNA strands with a contour length of 16.3 μm form complex extended structures (18). Depending on the local concentration of DNA and the exact preparation procedure, we observe thin DNA membranes and filamentous structures that occasionally bridge the holes of the support film (Fig. 1*A*). A crescent-shaped DNA sheet covers the lower part of a 2.5-μm diameter hole, with thin filaments (~20–30 nm diameter) extending to the top. Most of these nanostructures likely contain a mixture of different forms of DNA as well as ordered and amorphous domains.

Immediately after preparation, some DNA membranes showed selected area electron diffraction patterns, which are consistent with the B form of DNA (Fig. S1). While exposed to the low pressure in the microscope (1e-7 mbar), the structure of Fig. 1 had largely more time to dry, so we cannot draw definitive conclusions about the DNA form involved. We disconnected several filaments of the structure in Fig. 1*A* from the carbon support by cutting them with a focused electron beam. In the resulting structure (Fig. 1*B*), the free-standing filaments now slightly protrude from the plane of the carbon film, which is apparent from a tilt series (Movie S1). Furthermore, the DNA network connecting them to the crescent-shaped DNA sheet appears to have relaxed.

Author contributions: U.J.L. and A.H.Z. designed research, performed research, and wrote the paper.

The authors declare no conflict of interest.

[1]To whom correspondence should be addressed. E-mail: zewail@caltech.edu.

This article contains supporting information online at www.pnas.org/lookup/suppl/doi:10.1073/pnas.1300630110/-/DCSupplemental.

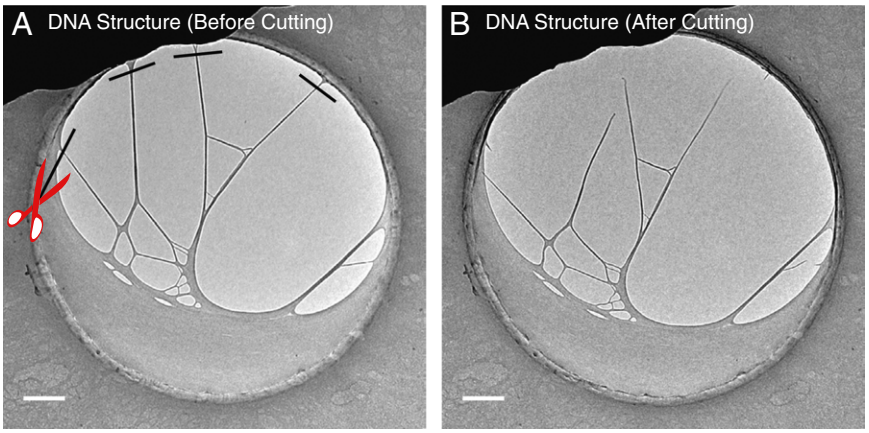

Fig. 1. Electron micrographs of the DNA nanostructure suspended over a hole of the support film. We cut several filaments in (*A*) with a focused electron beam to create a free-standing structure (*B*). (Scale bar, 300 nm.)

Vibrational Properties of the DNA Nanostructure. We investigated the vibrational properties of the DNA nanostructure of Fig. 1*B* by directly imaging the oscillatory motion that it undergoes, following impulsive excitation with a picosecond laser pulse at 532 nm. Fig. 2*A* displays stroboscopically recorded dark field images of the structure at $t_- = -100$ ns (i.e., 100 ns before the arrival of the excitation pulse), $t_1 = 40$ ns, and $t_2 = 110$ ns. A complete movie is provided in the Movie S2. The displacement of the filament on the left in the direction of arrow (a) is shown as a function of time in Fig. 2*B* (black curve). It exhibits fast, fairly regular oscillations, superimposed on a slow aperiodic motion, which is highlighted by a polynomial fit of the data (red). We also observe this slow, irregular movement without laser excitation and therefore ascribe it to a drift motion of the filament, which occurs on the timescale of the experiment (~1 h). Calibration experiments, whose results are provided in Fig. S2 and Table S1, indicate that the pulsed electron beam does not have a significant effect on this drift movement, suggesting a thermal origin for the drift. After subtraction of this thermal background from the horizontal movement (h) of the circled feature in Fig. 2*A*, the gray curve in Fig. 2*C* is obtained, which can be well approximated by a single sinusoidal function (blue). Using the same procedure, we obtained the oscillations for the filament labeled (a) in Fig. 2*A* and for other sites in the network. The frequency spectra of the data are similar after background subtraction except, of course, for the reduced intensity of low-frequency features.

Other calibration experiments show that the DNA nanostructures can deform over time, especially when the pump laser power is made relatively high; the pulsed electron beam did not seem to cause noticeable damage. We also investigated the effect of heating on the vibrational properties of the DNA structures. Despite some deformation that occurred after prolonged exposures to the pump laser beam, the vibrational frequencies of the investigated nanostructure remained unchanged to within 1%, whereas the vibrational amplitudes increased slightly.

We analyzed the vibrations of the DNA nanostructure of Fig. 1*B* by determining the deflection of the different filaments as a function of time (Fig. 3 *A*, arrows *a*–*d*) as well as the vertical (Fig. 3 *A*, *e* and *g*) and horizontal displacement (Fig. 3 *A*, *f* and *h*) of the circled features. A time–frequency analysis of the obtained transients is shown in Fig. 3*B*. It was carried out with the Multiple Signal Classification (MUSIC) algorithm (19) as implemented in

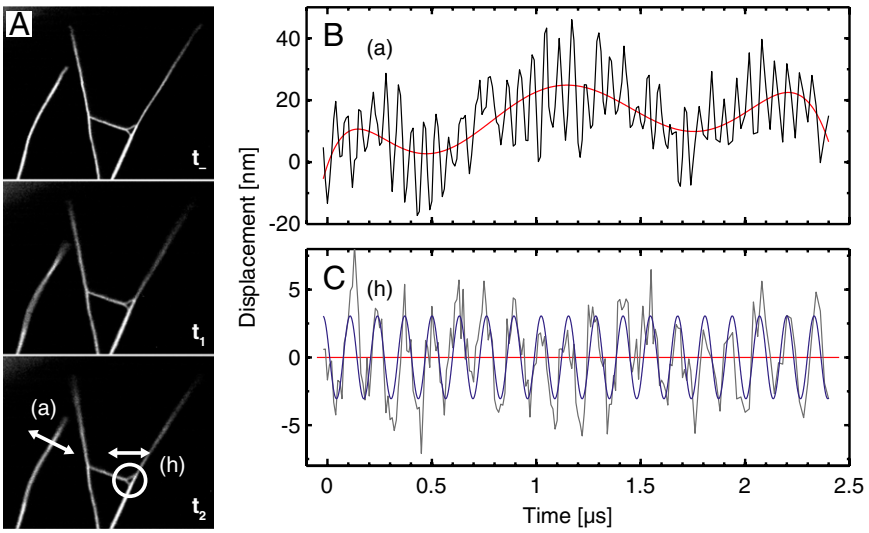

Fig. 2. Transient behavior of the DNA nanostructure following laser excitation. (*A*) Dark field UEM images recorded at $t_- = -100$ ns, $t_1 = 40$ ns, and $t_2 = 110$ ns. The displacement of the filament on the left in the direction of arrow (a) is shown in (*B*) as a function of time (black curve). A polynomial fit (red) highlights the underlying slow drift motion of the filament. With this underlying movement subtracted [gray curve in (*C*)], the horizontal displacement (h) of the circled feature can be well described by a simple sinusoidal function (blue curve).

MATLAB. Pseudospectra were calculated for 500-ns-long time windows and are displayed with a logarithmic intensity scale. The appearance of the spectra was found to be widely independent of the estimate of the signal subspace dimension; here an estimate of 23 was used (for 50 df).

The time–frequency analysis for the oscillations of the DNA filament on the left of Fig. 3*A* reveals a single oscillation frequency around 16.3 MHz (Fig. 3 *B*, *a* and *b*). At long times, the second harmonic appears in the pseudospectra, which is likely an artifact introduced by the lower sampling rate that was used after about 1.7 μs. The higher spectral resolution provided by the MUSIC algorithm [compared with, for example, a simple periodogram (19)] reveals that the oscillation frequency varies over time within a range of about 2 MHz; in particular, it prominently decreases around 0.75 μs. Independent of which part of the filament is monitored (Fig. 3 *B*, *a* and *b*), almost identical changes of the frequency are observed, which renders it unlikely that they could be explained as an artifact of the data analysis. Because the observed frequency variation is generally not reproducible, we conclude that it occurs on the timescale of the experiment, similar to the drift of the equilibrium position of the filament. However, both phenomena do not appear to be correlated.

The oscillation frequencies associated with the movement of the bifurcated structure on the right of Fig. 3*A* appear more stable (Fig. 3 *B*, *c*–*h*). By identifying frequencies common to different parts of the DNA nanostructure, we can attempt an assignment of its normal modes, which is illustrated in Fig. 3*C*. This analysis reveals that the ∼16 MHz oscillation of the single filament on the left of Fig. 3*A* is uncoupled from the rest of the structure. The double-headed arrow indicating the mode shape in Fig. 3*C* suggests an in-plane oscillation; however, we note that the oscillation might have an out-of-plane component that we cannot observe in projection. The bifurcated DNA structure exhibits two collective low-frequency oscillations. The entire branch swings in-plane with a frequency of ∼8 MHz, which is common to the deflection of the filaments (Fig. 3 *A*, *c* and *d*) and the horizontal displacement of the circled features (Fig. 3 *A*, *f* and *h*). Their vertical displacement (Fig. 3 *A*, *e* and *g*) shows a common ∼4 MHz oscillation, which indicates an out-of-plane motion of the branched structure. Furthermore, the loose ends of the branch (Fig. 3 *A*, *c* and *d*) exhibit oscillations with frequencies of ∼28 and ∼15 MHz, respectively. Whereas the weak ∼15 MHz vibration seems to be isolated, the ∼28 MHz oscillation is slightly delocalized and also appears weakly in the frequency spectra of the horizontal displacements (Fig. 3 *B*, *f* and *h*).

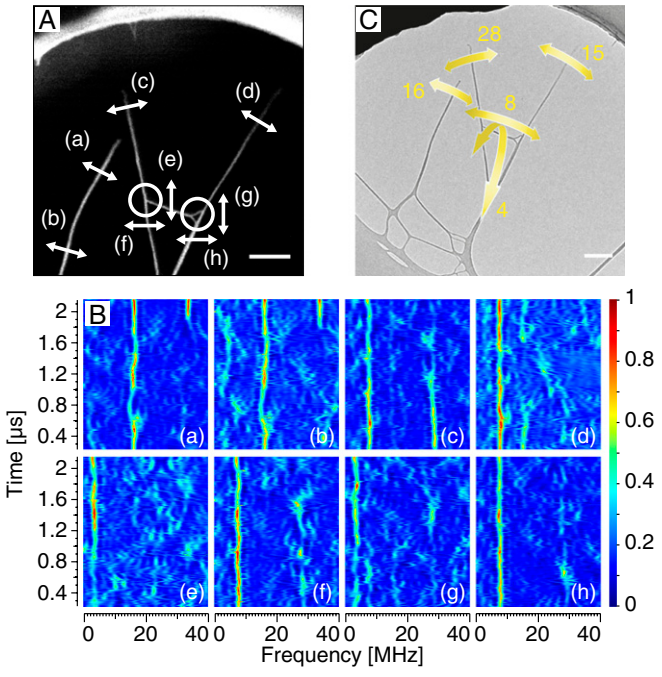

Fig. 3. Vibrational properties of the DNA nanostructure. As indicated in (*A*), the displacement of different filaments in the directions of arrows (*a*–*d*) is analyzed as a function of time as well as the vertical (*e* and *g*) and horizontal displacement (*f* and *h*) of the circled features. From the obtained transients, the slow drift motion of the structure is subtracted and a time–frequency analysis with the MUSIC algorithm is performed (*B*). The pseudospectra were obtained for 500-ns-long time windows and are shown with a logarithmic intensity scale. The shapes of the deduced vibrational modes of the DNA nanostructure are illustrated in (*C*), and their eigenfrequencies are given in megahertz. (Scale bars, 200 nm.)

The vibrational frequencies of the free-standing filaments can be used to obtain Young's modulus of the DNA structure. The filaments were approximated as prismatic beams of circular cross-section, clamped at one end and free at the other; their vibrations are largely isolated from the remaining structure (see the previous paragraph). For this cantilever case, Young's modulus, Y, can be obtained from the equation,

$$Y = \left(\frac{8}{\pi \cdot 1.194^2} \cdot \frac{f \cdot L^2}{\kappa}\right)^2 \cdot \rho,$$

where the frequency of the fundamental mode is f, the length of the beam is L, its density is ρ, the radius of gyration is κ = r/2, and r is the beam radius (20). When we determine L and r from Fig. 1*B* and assume the density ρ = 1.23 g/cm^3 of dehydrated DNA, as discussed in the following paragraph (21), we obtain a modulus of 15 ± 3 GPa for the isolated filament, as well as 12 ± 3 and 11 ± 3 GPa for the left and right filament of the bifurcated structure, respectively.

These values are considerably higher than the modulus of about 300 MPa that was determined in single-molecule stretching experiments in solution (6, 22). However, Brillouin scattering studies have previously found that at low levels of hydration, the modulus of DNA films strongly increases to values of 9.3–11.6 GPa at a relative humidity of 23% (21, 23). Our results are therefore consistent with a low level of DNA hydration, and this justifies our choice of the value for the density of DNA. Stiffening as a result of dehydration has been observed for different types of biological materials (8). In the case of DNA, it has been attributed to a combination of different effects. An increase of the strength of interhelical interactions appears to play an important role, which occurs when the distance between neighboring DNA strands decreases upon removal of interhelical water and the Coulomb interaction of their phosphate groups becomes stronger (21).

Excitation Mechanism. Close inspection of Fig. 2*A* reveals that the appearance of the single filament on the left changes with time. Although it appears sharp before time zero (t_-), the images at short times show strong blurring (t_1), which then decreases at later times (t_2). These images suggest the excitation of higher-order vibrational modes that manifest as image blurring before damping out. The broad band of frequencies excited at early times gives a hint to the nature of the excitation mechanism that we discuss here.

When an inhomogeneous cantilever such as a bimetallic nanostrip is heated, it acts as a thermostat (24). A laser-induced temperature jump will impulsively change its equilibrium position, so that it begins to oscillate (15). This excitation mechanism cannot be as effective for cantilevers consisting of homogeneous materials such as DNA. A sudden change of the equilibrium position leading to transverse oscillations can nevertheless be induced if the laser beam is sufficiently attenuated while passing through the cantilever and the material strongly expands or contracts as a result of photon absorption (25, 26). In this case, an

inhomogeneous strain profile is created along the direction of the laser beam, so that the cantilever starts to oscillate about its new equilibrium position.

Weakly absorbing, thin biological specimens would not lend themselves easily to this excitation mechanism, especially if they are sensitive to heat, and high pump laser powers must be avoided. Because DNA is transparent at visible wavelengths, we can exclude its direct excitation with the laser pulse. It is also unlikely that the strongly absorbing carbon substrate would rapidly heat the DNA structure and mediate a temperature jump. Using published values for the thermal conductivity (27), specific heat capacity (28), and density (21) of DNA, one can estimate that the DNA membrane, which connects the filaments to the carbon support, heats up on a timescale of about 100 ns after the substrate undergoes a temperature jump, far too slow to explain the oscillations of the filaments that set in promptly after the laser pulse.

To shed light on the excitation mechanism, we conducted the following series of experiments. The low-magnification image in Fig. 4*A* shows a DNA nanostructure (red circle) in the upper-left corner of a square area of the holey carbon film, which is surrounded by the copper bars of the support mesh. The distance between the DNA structure and the laser focus was successively increased. For each laser spot position (indicated by dots, with the surrounding circles representing the beam diameter of 40 μm), we recorded a movie covering the first 500 ns after laser excitation (Movie S3). An out-of-plane collective vibration of the tree-like DNA structure (Fig. 4*B*) was monitored by tracking the vertical displacement of the circled feature. This low-frequency mode is little affected by thermal drift motion, which is a prerequisite for the following analysis. Fig. 4*C* displays the displacement of the feature as a function of time for all eight laser spot positions, with two waveforms highlighted to correspond to the smallest and largest distance between the nanostructure and the laser focus. The data are presented with a three-point spline to reduce the amount of high-frequency noise.

In all eight experiments, we obtained waveforms of a similar shape, reminiscent of a driven oscillation, with the amplitude continually increasing during the first 500 ns. This behavior is inconsistent with a mechanism in which the pump laser pulse excites the DNA structure directly and induces oscillations (e.g., through inhomogeneous heating as discussed previously). In this case, one would expect the oscillation to reach its maximum amplitude immediately, as for example observed for microcantilevers of copper (7, 7, 8, 8-tetracyanoquinodimethane) (14). In our case here, a driving force persists for at least 500 ns after the laser pulse.

We propose that the oscillations of the DNA nanostructure are excited through vibrations of the holey carbon support that are triggered by the laser pulse. In fact, it has previously been reported that excitation of a 75-nm-thick single-crystalline graphite film with a 532-nm laser pulse induces drumming motions with frequencies in the megahertz range (12). Impulsive, local heating creates thermal stress, which initially leads to the excitation of vibrational modes with a broad band of frequencies. Rapid damping occurs, and at later times only a few modes persist. It is conceivable that the holey carbon film (a composite of a 10-nm layer of amorphous carbon on a 10-nm layer of organic polymer, supported by a copper mesh) should show a similar response to laser excitation, although we expect its oscillations to dampen out more rapidly because of the inhomogeneity of the material. Because the DNA nanostructure is mechanically connected to the

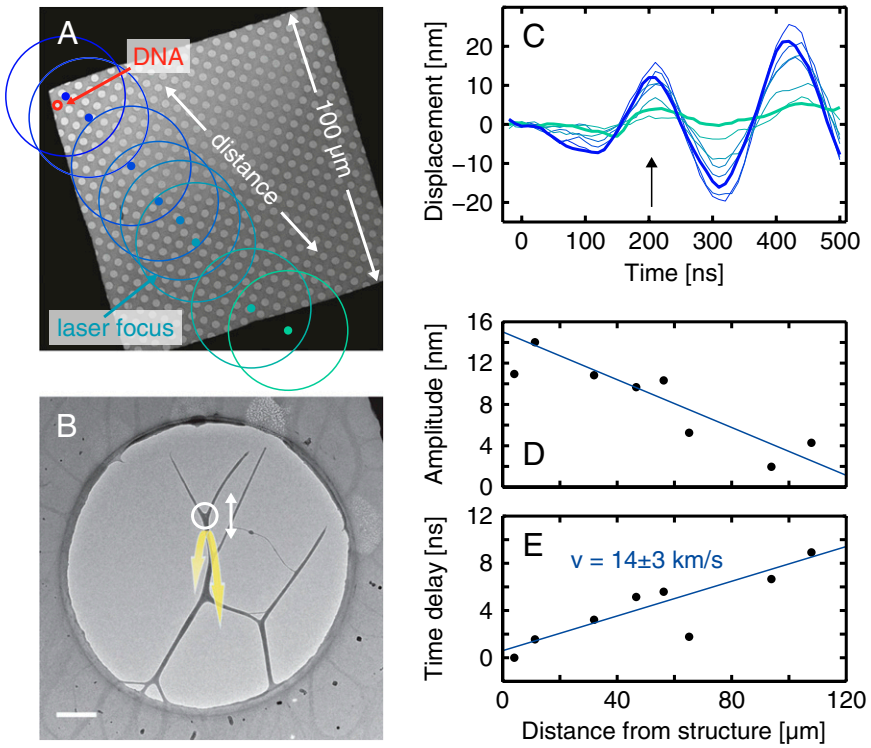

Fig. 4. Distance dependence of DNA mechanical vibrations. The out-of-plane vibration of the DNA nanostructure (*A*) is monitored by tracking the vertical displacement of the circled feature. (Scale bar, 300 nm.) The low-magnification micrograph (*B*) indicates the location of the structure (red circle) relative to the position of the laser focus (blue-green dots with the circles representing the beam diameter of 40 μm FWHM). The displacement of the tracked feature as a function of time is shown (*C*) for the different laser focus positions. The curves corresponding to the smallest and largest distance between structure and laser spot are highlighted. The amplitude and time delay of the first maximum (arrow) are extracted from a fit with a sinusoidal function and plotted as a function of the distance between structure and laser focus (*D* and *E*), respectively. From a linear fit to the data points (*E*), the speed of sound in the substrate is obtained to be $v = 14 \pm 3$ km/s.

support film, its eigenmodes will be excited if the frequency spectrum of the substrate vibrations covers the range of their eigenfrequencies (29). That oscillations of the DNA structure are excited even though the laser focus is positioned at a distance of more than 100 μm (whereas the laser spot diameter is only about 40 μm) lends further support to the proposed excitation mechanism. Evidently, the carbon substrate transfers the excitation energy to the structure.

For the purpose of a quantitative analysis, we measured the distance between the structure and the laser focus in μm and determined the amplitude in nanometers and time delay in nanoseconds of the first maximum of the vibrational waveform (marked with an arrow in Fig. 4*C*) from a fit with a sinusoidal function. We can thus determine the spatial extent of the induced vibrations (stress) in the substrate as well as their speed of propagation. As shown in Fig. 4*D*, the amplitude decreases as a function of the distance, which supports the notion that the oscillations of the holey carbon film have their maximum amplitude at the center of the laser spot where the thermal stress is greatest. The time delay of the oscillation increases with distance (Fig. 4*E*). From a linear fit (blue line), the speed of sound in the holey carbon film was deduced giving $v = 14 \pm 3$ km/s, which agrees favorably with the speed of 8.7–14 km/s (30) measured in amorphous carbon thin films. This result further supports the suggested acoustic excitation mechanism; the laser pulse induces a short burst of strain vibrations in the substrate, which in turn impulsively excite mechanical oscillations of the structure of interest.

Conclusions

We have demonstrated the nanoscale imaging of the biomechanics of DNA structures. Our approach enables the determination of vibrational normal modes and eigenfrequencies as well as Young's modulus of free-standing DNA filaments that exhibit isolated oscillations. The mechanical oscillations of the DNA structure are excited through vibrations of the holey carbon following an impulsive excitation with a clocking laser pulse, even at a distance from the DNA structure. This excitation scheme avoids photodamage, because it does not require photon absorption of the DNA itself and the excitation can be made tens of microns away from the structure. The pulsed electron beam did not induce damage, possibly because of its short duration relative to the repetition rate. Last, the values obtained for Young's modulus indicate that the DNA structure is fairly dehydrated. An environmental cell should allow one to control the level of hydration. With this first report, we demonstrate that our technique, building on the capabilities of 4D electron microscopy, can visualize the mechanics of complicated nanoscopic structures in space and time and should be applicable in the study of other biological nanomaterials.

Materials and Methods

DNA nanostructures were prepared as previously described (31). A solution of λ-DNA (Takara Bio Inc.; 200–500 μg/mL, 10 mM Tris·HCl, pH 8.0, 1 mM EDTA) was diluted by a factor of 50 with deionized water (with a resistivity of 18 MΩcm at 25 °C), of which a 5-μL drop was placed onto a Quantifoil holey carbon film with 2.5-μm-diameter holes that had been rendered hydrophilic in an argon/oxygen plasma. After incubating for 5 min, the solution was wicked away with filter paper and the sample was washed twice with 3 μL of deionized water before it was allowed to dry.

The resulting DNA nanostructures were imaged and manipulated by electron beam cutting in our UEM-1 (10). Time-resolved experiments were carried out in stroboscopic acquisition mode as described previously (32). Briefly, the vibrational dynamics of the DNA nanostructures were triggered with 532-nm picosecond laser pulses that were focused onto the specimen (16-ps FWHM, 0.25-μJ pulse energy, 40-μm FWHM spot size). A 266-nm nanosecond laser (10-ns FWHM), synchronized to the pump laser with a digital delay generator (25-ns jitter), produced photoelectron pulses that were used to image the structure at a given delay after excitation. Frames recorded every 10 or 20 ns were then used to construct a movie. Experiments were carried out with a repetition rate of 1 kHz (which ensured that oscillations had subsided before the beginning of the next cycle) and an acquisition time of 15 s per frame. Images were recorded in centered dark field mode, with the tilt angle of the incident electron beam optimized for maximum contrast.

Cross-correlation–based image registration was used to align the movie frames relative to each other as well as to track the branching points of DNA structures. The deflection of filaments along a given line was determined by obtaining an intensity profile and fitting it with a Gaussian. For the analysis of the excitation mechanism, the position of the laser focus was determined by recording microscopic burns on a Quantifoil holey carbon film. The extrema of the vibrational waveforms in Fig. 4*C* were fit to the function,

$$y = a + (b_0 + b_1 t) \cdot \sin(\omega t + \Phi),$$

where y is the displacement, t the time, and a, b_0, b_1, ω, and Φ are fit parameters. For the determination of Young's modulus, we obtained the length of the filaments from Fig. 1*B* by measuring the distance from their tip to their point of attachment to the nanostructure. Because they slightly protrude from the plane of the holey carbon film, we are bound to somewhat underestimate their length. Their radii were determined from intensity profiles measured orthogonal to the filament tangent along its entire length. The profiles were aligned with respect to each other using the cross-correlation methodology. With this procedure, we obtain an average of the radius, which slightly varies over the length of the filament.

ACKNOWLEDGMENTS. We thank Professors Charles M. Lieber, Chad A. Mirkin, Carlos Bustamante, and John M. Thomas for insightful remarks, as well as Dr. S. T. Park for helpful discussions. This work was supported by the National Science Foundation Grant DMR-0964886 and Air Force Office of Scientific Research Grant FA9550-11-1-0055 in the Physical Biology Center for Ultrafast Science and Technology at Caltech supported by the Gordon and Betty Moore Foundation. U.J.L. is grateful for a postdoctoral fellowship from the Swiss National Science Foundation.

1. Lu W, Lieber CM (2007) Nanoelectronics from the bottom up. *Nat Mater* 6(11): 841–850.
2. Jones MR, Mirkin CA (2012) Materials science: Self-assembly gets new direction. *Nature* 491(7422):42–43.
3. Bath J, Turberfield AJ (2007) DNA nanomachines. *Nat Nanotechnol* 2(5):275–284.
4. Aldaye FA, Palmer AL, Sleiman HF (2008) Assembling materials with DNA as the guide. *Science* 321(5897):1795–1799.
5. Pinheiro AV, Han DR, Shih WM, Yan H (2011) Challenges and opportunities for structural DNA nanotechnology. *Nat Nanotechnol* 6(12):763–772.
6. Bustamante C, Bryant Z, Smith SB (2003) Ten years of tension: Single-molecule DNA mechanics. *Nature* 421(6921):423–427.
7. Bustamante C, Smith SB, Liphardt J, Smith D (2000) Single-molecule studies of DNA mechanics. *Curr Opin Struct Biol* 10(3):279–285.
8. Ebenstein DM, Pruitt LA (2006) Nanoindentation of biological materials. *Nano Today* 1(3):26–33.
9. Zlatanova J, Lindsay SM, Leuba SH (2000) Single molecule force spectroscopy in biology using the atomic force microscope. *Prog Biophys Mol Biol* 74(1-2):37–61.
10. Zewail AH, Thomas JM (2010) *4D Electron Microscopy: Imaging in Space and Time* (Imperial College Press, London).
11. Zewail AH (2010) Four-dimensional electron microscopy. *Science* 328(5975):187–193.
12. Kwon O-H, Barwick B, Park HS, Baskin JS, Zewail AH (2008) Nanoscale mechanical drumming visualized by 4D electron microscopy. *Nano Lett* 8(11):3557–3562.
13. Kwon O-H, Zewail AH (2010) 4D electron tomography. *Science* 328(5986):1668–1673.
14. Flannigan DJ, Samartzis PC, Yurtsever A, Zewail AH (2009) Nanomechanical motions of cantilevers: Direct imaging in real space and time with 4D electron microscopy. *Nano Lett* 9(2):875–881.
15. Baskin JS, Park HS, Zewail AH (2011) Nanomusical systems visualized and controlled in 4D electron microscopy. *Nano Lett* 11(5):2183–2191.
16. Middleton CT, et al. (2009) DNA excited-state dynamics: From single bases to the double helix. *Annu Rev Phys Chem* 60:217–239.
17. Fu Z-F, He J (2001) *Modal Analysis* (Butterworth-Heinemann, Oxford).
18. Fink HW, Schönenberger C (1999) Electrical conduction through DNA molecules. *Nature* 398(6726):407–410.
19. Castanié F (2006) *Spectral Analysis: Parametric and Non-Parametric Digital Methods* (ISTE Ltd., London).
20. Kinsler LE, Frey AR, Coppens AB, Sanders JV (2000) *Fundamentals of Acoustics* (John Wiley & Sons, Inc., New York).
21. Lee SA, et al. (1987) A Brillouin scattering study of the hydration of Li- and Na-DNA films. *Biopolymers* 26(10):1637–1665.
22. Smith SB, Cui Y, Bustamante C (1996) Overstretching B-DNA: The elastic response of individual double-stranded and single-stranded DNA molecules. *Science* 271(5250): 795–799.
23. Hartschuh RD, et al. (2008) How rigid are viruses. *Phys Rev E Stat Nonlin Soft Matter Phys* 78(2 Pt 1):021907.
24. Timoshenko S (1925) Analysis of bi-metal thermostats. *J Opt Soc Am Rev Sci* 11(3): 233–255.

25. Yu YL, Nakano M, Ikeda T (2003) Photomechanics: Directed bending of a polymer film by light. *Nature* 425(6954):145–145.
26. Warner M, Mahadevan L (2004) Photoinduced deformations of beams, plates, and films. *Phys Rev Lett* 92(13):134302.
27. Savin AV, Mazo MA, Kikot IP, Manevitch LI, Onufriev AV (2011) Heat conductivity of the DNA double helix. *Phys Rev B* 83(24):245406.
28. Privalov PL (2012) *Nucleic Acids. Microcalorimetry of Macromolecules: The Physical Basis of Biological Structures* (John Wiley & Sons, Inc., Hoboken).
29. Rubin S, Ahlin K (2010) *Harris' Shock and Vibration Handbook*, eds Piersol AG, Paez TL (McGraw-Hill, New York), pp 20.1–20.23.
30. Bullen A, O'Hara K, Cahill D, Monteiro O, von Keudell A (2000) Thermal conductivity of amorphous carbon thin films. *J Appl Phys* 88(11):6317–6320.
31. Germann M, Latychevskaia T, Escher C, Fink H-W (2010) Nondestructive imaging of individual biomolecules. *Phys Rev Lett* 104(9):095501.
32. Park ST, Flannigan DJ, Zewail AH (2012) 4D electron microscopy visualization of anisotropic atomic motions in carbon nanotubes. *J Am Chem Soc* 134(22):9146–9149.